scientific reports

OPEN

Predicted thermodynamic structural and elastic properties of SrCuP and SrCuSb for thermoelectric applications

N. Bioud[1,2]✉, N. Benchiheub[3], A. Benamrani[3], M. A. Ghebouli[4,5], M. Fatmi[4]✉, Faisal Katib Alanazi[6]✉ & R. Yekhlef[7,8]

The Pseudopotential method coupled with plane waves implemented in the quantum espresso code was used in the prediction of the structural parameters and elastic constants of SrCuX (X = P, Sb) materials. The obtained results of lattice parameters and bulk modulus at equilibrium agree well with their experimental and theoretical data cited in the literature. The calculated Young's modulus of SrCuX (X = P, Sb) aggregate thermoelectric materials are 109.25 GPa and 78.22 GPa, while their Debye temperatures are 364.2 K and 261.8 K. The vibration energy of phonons is 24.14 kJ/mol and 23.37 kJ/mol for SrCuP and SrCuSb. Our thermodynamic parameters increase monotonically with temperatures for both SrCuP and SrCuSb materials. To the best of our knowledge, there are no data available in the literature on the elastic and thermodynamic parameters of SrCuX (X = P, Sb) compounds, then our results are prediction. The absence of virtual phonon frequencies indicates high dynamic stability in both materials, with a band gap about 1 THz between optical and acoustic phonons in SrCuP and SrCuSb.

Keywords Ab-initio calculations, Elastic properties, SrCuX (X = P, Sb) thermoelectric materials, Thermo_pw package, Thermodynamic properties

Theoretical methods integrating first-principle calculations have constantly progressed in recent years[1]. Using always faster computers and more efficient computer codes, these approaches allow the investigation of a large set of materials (elements, compounds, alloys,.etc.) in a much shorter time than experiments[1]. First-principles calculations based on the density functional theory are one of the most powerful tools to understand the physical properties of materials[2]. For example, these calculations can provide information about spin distribution in magnetic materials which are not measured from experiment[2]. The interest in the equimolar composition TMX intermetallic compounds (where *T* is a transition metal from the Ti, V, Cr columns, Sr, Ba, Y and La, *M* an element from the first line of transition metals, while *X* is a *sp* elements: Al, P, Si, Sn, and Sb)[1] was started a long time ago. Using X-ray methods, Mewis[3] has studied the crystal structure of some ternary phosphides and arsenides intermetallic compounds. They mentioned that all CaCuP, CaCuAs, SrCuP, SrCuAs, SrAgP, SrAgAs and EuCuAs compounds crystallize in a modified Ni_2In structure (space group $P6_3/mmc\text{-}D^1_{6h}$), while Eisenmann et al.[4] have investigated experimentally the structural parameters of the ternary CaCuSb, CaCuBi, SrCuSb and SrCuBi compounds. Very recently, several interesting aspects of TMX compounds have been computed and measured. Barreteau et al.[1] found that the SrCuSb compound is non-metallic in the BeZrSi structure-type ($P6_3/mmc$ (N° 194) space group), while Moll et al.[5] have investigated the thermoelectric properties of SrCuX (X = P or Sb) experimentally and with the density functional theory (DFT) calculations. Moll et al.[5] have

[1]Faculty of Sciences and Technology, University of Mohamed El Bachir El Ibrahimi-Bordj Bou Arreridj, 34000 Bordj Bou Arreridj, Algeria. [2]Laboratory of Optoelectronic and Compounds, Faculty of Sciences, Ferhat Abbas University of Setif 1, 19000 Setif, Algeria. [3]Laboratory of Materials Physics, Radiation and Nanostructures (LPMRN), University of Mohamed El Bachir El Ibrahimi-Bordj Bou Arreridj, 34000 Bordj Bou Arreridj, Algeria. [4]Research Unit On Emerging Materials (RUEM), University Ferhat Abbas of Setif 1, 19000 Setif, Algeria. [5]Department of Chemistry, Faculty of Sciences, University of Mohamed Boudiaf, 28000 M'sila, Algeria. [6]Department of Physics, College of Sciences, Northern Border University, Arar, Saudi Arabia. [7]Research Center in Industrial Technologies CRTI, P.O. Box 64, 16014 CheragaAlgiers, Algeria. [8]Laboratory of Electrochemistry, Molecular Engineering and Redox Catalysis (LEIMCR) Department of Engineering Process, Faculty of Technology, Ferhat Abbas University Setif-1, 19000 Setif, Algeria. ✉email: nadhira.bioud@univ-bba.dz; fatmimessaoud@yahoo.fr; Faisal.katib.al@gmail.com

mentioned that both SrCuP and SrCuSb compounds are stable and non-metallic, and these two non-metallic compounds are suitable for thermoelectric applications. They have mentioned also that some equimolar *TMX* compounds can also crystallize in other structure types such as the hexagonal BeZrSi type. Quinn and Bos[6] have studied the thermoelectric parameters of several phosphide materials promising for thermoelectric conversion. Furthermore, they have also reported theoretically on the gravimetric density, bulk and shear moduli, sound velocity, Debye temperatures, and Grüneisen parameters using the Materials Project computer software[7]. In other work[8], they have reported on electronic band structure information, thermal transport properties, and several other thermoelectric properties of some selected half-Heusler alloys.

Using vacuum induction melting method, Zheng et al.[9] developed a series of planar Zintl-phase XCuSb (X = Ca, Sr, Ba) thermoelectric materials. Using experimental measurements and theoretical calculations, Zheng et al.[9] found that all these thermoelectric compounds exhibit high carrier mobilities and intrinsic low lattice thermal conductivities. Knowledge of mechanical and thermodynamic properties of materials is very important for many technological applications[10–18]. Despite the importance of the mechanical and thermodynamic properties of SrCuP and SrCuSb materials, only some data have been carried out on the physical properties of SrCuSb compound[11]. The thermoelectric materials have small band gap. The thermoelectricity enables the direct conversion of heat into electricity[19]. The efficiency of the thermoelectricity is governed by the figure of merit, which is related to the Seebeck coefficient, electrical resistivity and thermal conductivity. The main applications of thermoelectricity consist of medical devices, wearables, energy sensors and microelectronics. An experimental study of SrCuX (X = P, Sb) Zintl phases confirms their stability and non-metallic character, which are favorable as potential thermoelectric materials[20]. Thermoelectric analysis of Co_2TiX(X = Al, Ga, In, Si, Ge, Sn) compounds showed a figure of merit close to unity, this makes them potential in thermoelectric applications[21–24]. The obtained results on both L21 and XA phases ordering of Ti_2FeGe indicate their candidate as optoelectronic and spintronic applications[25]. Both L21 and XA ordering of Co_2FeGe compounds exhibit a ferromagnetic metallic nature[26]. The thermoelectric and thermal properties of $Co_2FeGa_{1-x}Si_x$ with concentration range $0 \le x \le 1$ exhibit half-metallic and metallic character[27]. The ferromagnetic material Ni_2MnGa shows a semi-metallic characteristic with a Curie temperature approximately 358 K and thus is considered a promising candidate for incorporation into spintronic devices[28].

In the present work, we report on first-principle calculations of the structural parameters, elastic constants, and thermodynamic parameters of SrCuP and SrCuSb compounds. Our findings are analyzed and compared to other data available from the literature. The SrCuX (X = P, Sb) compounds are highlighted to obtain new materials with adequate thermoelectric characteristics, such as their figure of merit and dynamic and thermodynamic stability.

Method of calculation

Both the pseudopotential and all-electron calculations were performed from first principles, based on DFT. The pseudopotential calculations were performed using Quantum Espresso code[29,30]. The calculations were carried out using A PAW pseudopotential[31] with a cut-off radius of 0.75 a.u, with the sg15 optimized norm-conserving Vanderbilt (ONCV) pseudopotentials[32]. PAW method considers a plane-wave basis set, but augmented in the region near the nucleus to describe the atomic-like wave function. The exchange–correlation effects were described using the generalized gradient approximation (GGA), according to the Perdew–Burke–Ernzerhof[33]. Convergence tests 57.5 and 345.5 Ry for the plane-wave basis-set cutoffs energy for the wave function and charge density, respectively. Wave functions were expanded with an energy cutoff of 90 Ry for SrCuP and 110 Ry for SrCuSb, respectively, which conduct to a convergence threshold of 1.0×10^{-4} Ry. Integration over the Brillouin zone was performed using Monkhorst–Pack grids[34] of 6 × 6 × 3 and 8 × 8 × 4 for SrCuP and SrCuSb, respectively.

Results and discussion

Equation of state (EoS) parameters

In order to determine the structural parameters of SrCuP and SrCuSb ternary compounds, which crystallize in the BeZrSi structure-type with space group ($P6_3/mmc$-D^1_{6h}(N° 194) as shown in Fig. 1. The equilibrium lattice parameters *a* and *c* were calculated using volume cell relaxation with the Broyden–Fletcher–Goldfarb–Shannon (BFGS) algorithm[35–39], which is implemented in Quantum Espresso code. The procedure of finding the unit cell volume V_0, the bulk modulus B_0 and its pressure derivative $B_0^{'}$ is from the fit of energy-volume (*E*-*V*) data using the Murnaghan's equation of state (M-EOS)[13,16] given by:

$$E\left(V\right) - E\left(V_0\right) = \frac{B_0 V}{B_0\prime}\left[\frac{\left(V_0/V\right)^{B_0\prime}}{B_0\prime - 1} + 1\right] - \frac{B_0 V_0}{B_0\prime - 1} \tag{1}$$

where E_0 is the energy of the ground state, corresponding to the equilibrium volume V_0.

Figure 2**;** shows the variation of the total energy *E* as a function of the unit cell volume *V* for SrCuP and SrCuSb ternary compounds. The calculated values of equilibrium parameters a_0, c_0, V_0, B_0, and $B_0^{'}$ are summarized in Table 1, with their experimental results[3–5] and other calculations[5,11,40]. The compounds SrCuP and SrCuSb investigated by X-ray diffraction are isotypic and crystallize in a modified Ni_2In structure (space group $P6_3$/mmc-D^1_{6h}) have the lattice parameters $a = 4.146$ Å $c = 8.376$ Å[3] and 4.527 Å $c = 8.752$ Å[5]. The obtained results of lattice parameters and bulk modulus at equilibrium state agree well with their experimental[5] and theoretical[3–5,11,40] data cited in the literature. These results demonstrate the effectiveness of the calculations in this work. The

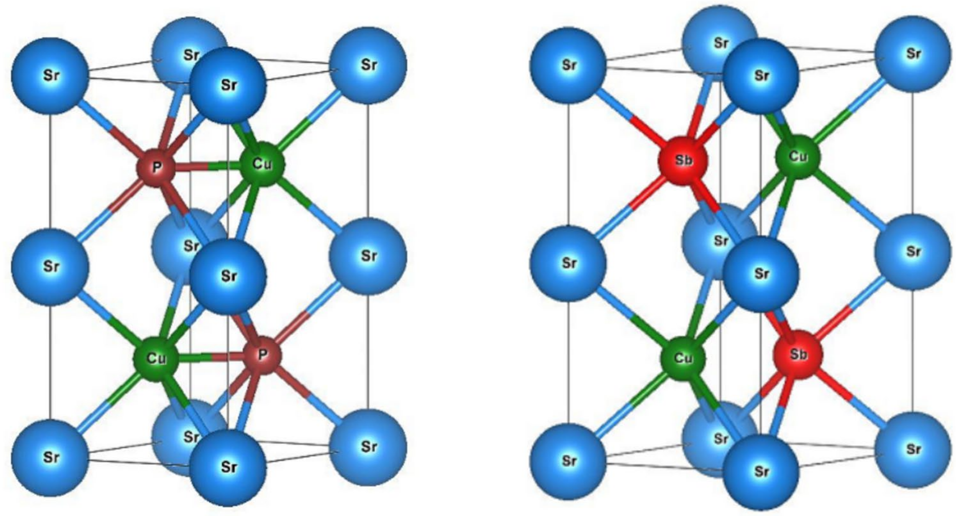

Fig. 1. Unit cells of SrCuP and SrCuSb compounds in the BeZrSi type-structure.

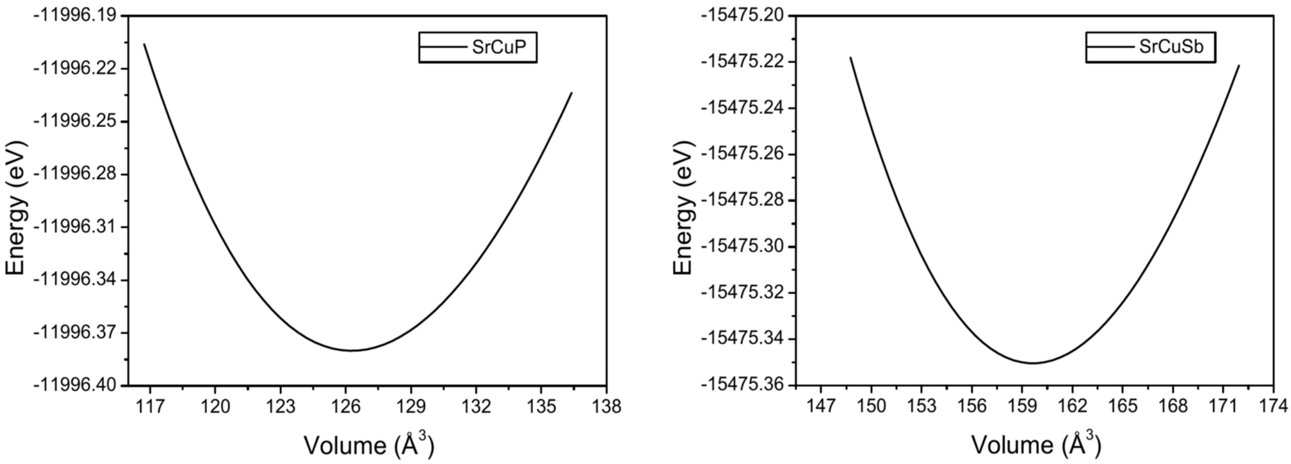

Fig. 2. Total energy *E* versus unit cell volume *V* for SrCuX (X = P, Sb) compounds in the BeZrSi type-structure.

EOS parameter	$a_0 = b_0$ (Å)	c_0 (Å)	V_0 (Å^3)	B_0 (GPa)	B'_0
SrCuP	4.1134[a]	8.5934[a]	125.92[a],	66.55[b]	4.57[b]
Exp	4.146[3,5] Exp	8.376[3], 8.382[5]	124.78[5] 126.28[b]	62.00[40]	
Other	4.138[5]	8.541[5]			
SrCuSb	4.5424[a]	8.8929[a]	158.91[a], 155.33 [5] 158.866[11]	49.99[b]	4.57[b]
Exp	4.527[5]	8.752[5]	159.64[b]	43.92[40]	
Other	4.547[5], 4.540[11]	8.926[5]			
	4.52[4]	8.900[11]			

Table 1. EOS parameters for both SrCuP and SrCuSb compounds, in comparison with others data from the literature. [a]This work using the BFGS algorithm, [b]This work using M-EOS.

deviations between our values of V_0 and the experimental ones reported in reference[5] are around 0.91% for SrCuP and 2.3% for SrCuSb compound, respectively.

Regarding the effect of the spin state on the total energy of the system and the calculated properties, Calculations of energy versus volume for each compound in possible feromagnetic, antiferamagnetic and non-magnetic states were investigated. The curves were identical (superimposed on each other), which is proof of the negligible effect of the magnetic state.

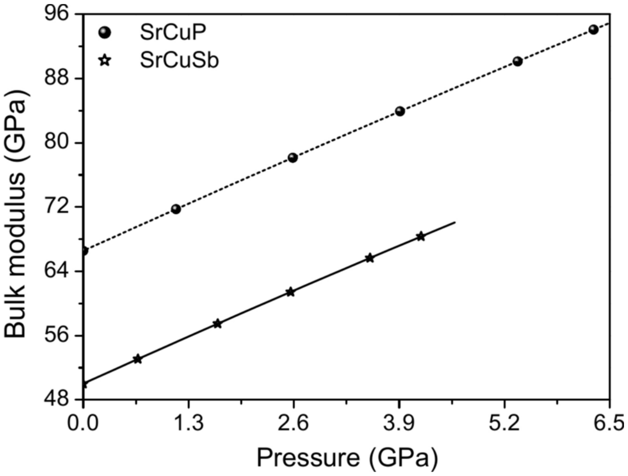

Fig. 3. Pressure dependence of the bulk modulus B for SrCuP and SrCuSb compounds.

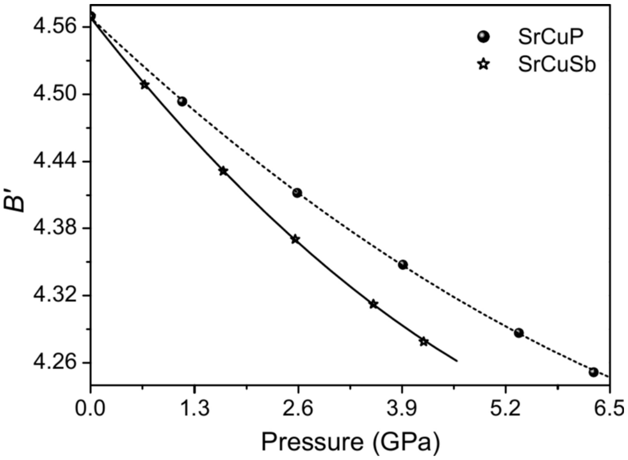

Fig. 4. Pressure derivative of the bulk modulus B′ versus pressure for SrCuX (X = P, Sb) materials.

Other factors that might contribute to discrepancies are temperature variations: DFT provides a zero-temperature description of the state of the material, whereas many experiments are done at room temperature.

Based on the compressibility β of material, a simple and efficacy expression has been used to calculate the hardness H of several mineral materials, this simple expression is given by the following relationship[41]:

$$H = \frac{M}{\rho q \beta} \tag{2}$$

where M is the molecular weight, ρ is the gravimetric density, and q is the number of atoms in a formula unit.

Using the previous relationship, the estimated values of the hardness are around 8.43 GPa for SrCuP and 8.01 GPa for SrCuSb, respectively. This later value is in good agreement with the theoretical one (H_V=7.73 GPa) reported in reference[11]. The deviation between the two values is around 3.62%. No data on the hardness H could be found in the literature to make a comparison for SrCuP material.

Recently some interesting works[17,18] have studied the variation of the isothermal bulk modulus B and its first pressure derivative B' as a function of pressure using some analytical expressions. Based on the expressions established by Mahammed and Mohammed[18], the variation of the isothermal bulk modulus B and its first pressure derivative B' as a function of pressure for SrCuP and SrCuSb compounds are shown in Figs. 3 and 4, respectively. The bulk modulus of both compounds increases gradually with increasing pressure, while the pressure derivative of B decreases with raising pressure. The increase in bulk modulus with pressure may be for the reason that pressure decreases the unit cell volume which, in turn, decreases the interatomic distance and hence an increase in bulk modulus occurs. Similar qualitative behaviors have been reported for $LiMAl_2$

C_{ij} GPa)	C_{11}	C_{12}	C_{13}	C_{33}	C_{44}	C_{66}
SrCuP	145.69^a	31.06^a	38.24	96.69	38.67	57.32
SrCuSb	112.87^a 127.79[11]	32.45^a 31.72[11]	24.77 23.88[11]	61.21 58.43[11]	27.63 28.27[11]	40.21 47.99[11]

Table 2. Elastic constants C_{ij} (in GPa) of SrCuP and SrCuSb compounds.

Parameter	B (GPa)	G (GPa)	E (GPa)	v	$k = G/B$
SrCuP	66.28	44.58	109.25	0.23	0.67
SrCuSb	47.77 48.88[11]	31.87 34.82[11]	78.22 84.42[11]	0.23 0.21[11]	0.67 0.71[11]

Table 3. Bulk modulus B, shear modulus G, Young modulus E, Poisson's ratio v, and Pugh's ratio $k = G/B$ for SrCuP and SrCuSb compounds.

(M = Rh, Pd, Ir and Pt) ternary compounds[16], for calcium oxide (CaO) binary compound[17] and for nine element materials[18].

Elastic constants and their related parameters

The elastic stiffness constants are essential parameters that can provide a link between the mechanical and dynamic behavior of crystals[13]. Furthermore, they give important information on the nature of the chemical bonding operating in solids[13]. The elastic stiffness tensor of hexagonal crystals is characterized by five independent elastic constants: C_{11}, C_{12}, C_{13}, C_{33} and C_{44} [11,13], while the elastic constant C_{66} is expressed as a function of the elastic stiffness constants C_{11}, C_{12} as follows: $C_{66} = (C_{11}\text{-} C_{12})/2$[11,42]. Nesa Rima et al.[11] mensioned that there is correlation between C_{44} and the material hardness H, where the higher value of C_{44} indicates more hardness H. Our results regarding the elastic constants C_{ij} of both SrCuP and SrCuSb compounds are listed in Table 2. The elastic constants for the hexagonal crystals should satisfy the following stability criteria[13]:

$$C_{11} > 0, C_{44} > 0, (C_{11} - C_{12}) > 0, \quad \text{and } (C_{11} + C_{12})C_{33} > \tag{3}$$

In addition to these stability criteria, Nesa Rima et al.[11] added another condition, $C_{33} > 0$. Clearly, according to the results shown in Table 2, the elastic constants of both SrCuP and SrCuSb crystals obey above the mechanical stability conditions. Then, our elastic constants in the hexagonal structure ensure the mechanical stability of these two compounds. Our data on the elastic constants C_{ij} for SrCuSb crystal are in agreement with the results reported in reference[11]. To the best of the authors' knowledge, no data on the elastic constants C_{ij} are available in the literature to make the comparison for SrCuP compound.

We know that the Voigt-Reuss-Hill (VRH) approximation is often used for the aggregate polycrystalline materials[13]. All details on the VRH approach for hexagonal structure are reported in reference[13]. Young's modulus E and Poisson's ratio v are calculated using bulk modulus B and shear modulus G by the following expressions: $E = 9BG/(3B + G)$, and $v = (3B\text{-}2G)/(6B + 2G)$[13,43,44]. Our obtained values of the bulk modulus B, shear modulus G, Young's modulus E, Poisson's ratio v, and Pugh's ratio ($k = G/B$) for both SrCuP and SrCuSb compounds are listed in Table 3. The calculated Young's modulus E for the aggregate SrCuP material is around 109.25 GPa, which is much larger than the value 78.22 GPa reported for SrCuSb compound. Our data on the elastic moduli for SrCuSb are slighly lower than the results reported in Reference[11]. For SrCuSb compound, the deviation between our value (78.22 GPa) of E and the theoretical one (84.42 GPa) reported in reference[11] is around 7.34%. No data on the elastic moduli could be found in the literature to make a comparison for SrCuP. To predict the ductile–brittle nature of materials, the Poisson's ratio v is often used. If the value of $v < 0.26$, thus implies the brittle manner behavior of the compound, while if $v > 0.26$, this implies the ductile behavior of the material[16,44]. One can see that all the values of v are (~ 0.23) to be smaller than 0.26 implying both SrCuP and SrCuSb compounds behave in a brittle manner at normal conditions. This conclusion on brittle behavior for both SrCuP and SrCuSb compounds could be confirmed also from the values of Pugh's ratio ($k \sim 0.67 > 0.57$)[16,44]. This behaviour was also observed for some ACuSb (A = Ca, Sr, Ba) ternary intermetallic materials[11]. Because there is a direct correlation between the elastic moduli and the hardness, usually, the search for a material's hardness is made easier by seeking materials with substantial bulk or shear moduli[11]. The Vickers hardness H_V is very largely dependent to dislocations and other defects of the solid[16], one of the expressions related Vickers hardness H_V and the elastic moduli is giveen as follows[45]:

$$H_V = 0.92k^{1.137}G^{0.708} \tag{4}$$

Our calculated results for the Vickers hardness H_V are 8.58 GPa for SrCuP and 6.77 GPa for SrCuSb, respectively. The first value (8.58 GPa) of H_V is in excellent agreement with the result (8.43 GPa) obtained from the formula of Eq. (2), while the second one (6.77 GPa) is lower than that (8.01 GPa) obtained from the expression of Eq. (2). An anisotropy index informs on the degree of which a system's properties are directionally dependent. To provide an accurate measure of anisotropy, the universal anisotropy factor (A^U) was often used. Since A^U may apply to all the crystal symmetries, it is referred to as universal anisotropy factor; it can be written as[15]:

$$A^U = 5\frac{G_V}{G_R} + \frac{B_V}{B_R} - 6 \geq 0 \tag{5}$$

For isotropic material, A^U is zero[15]. The non-zero values (~ 0.26 for SrCuP and ~ 0.39 for SrCuSb, respectively) of A^U indicate the anisotropic nature of both SrCuP and SrCuSb compounds, which becomes higher with the replacement of P element by Sb one.

Acoustic wave speeds, acoustic impedance and Debye temperature

The Debye temperature θ_D is a fundamental thermodynamic property used to distinguish between low and high temperature regions for a solid[16,44,46]. At low temperatures, it can be predicted from the average acoustic wave velocity v_m using the following expression[16,44]:

$$\theta_D = \frac{\hbar}{k_B}\left[\left(\frac{6\pi^2 NK}{V}\right)\right]^{1/3} v_m \tag{6}$$

Where $\hbar = h/2\pi$, h is the Planck constant; k_B is the Boltzmann constant, N is the number of unit cells in the volume V of the crystal, and K is the number of atoms per unit cell.

The values of the longitudinal, transverse, and average acoustic wave speeds and the Debye temperature θ_D for both SrCuP and SrCuSb materials are listed in Table 4. More details on the calculation of the acoustic wave speeds and the Debye temperatures from the Debye's approach, please see the references[44,46]. The calculated value of the Debye temperature θ_D is 364.2 K for SrCuP, which is higher than the value 261.8 K reported for SrCuSb compound. This explains that Debye temperature θ_D correlates with the Young's modulus E ($E = 109.25$ GPa for SrCuP is higher than $E = 78.22$ GPa reported for SrCuSb). According to Reference[14], a larger θ_D value suggests a higher normal vibration, which is associated with better thermal conductivity. Such as Young's modulus E, our Debye temperature (261.8 K) for SrCuSb is slighly lower than the theoretical result (272.5 K) reported in Reference[11]. To the best of authors' knowledge, there are no experimental or other theoretical data available in the literature on the acoustic wave speeds and the Debye temperature θ_D for SrCuP material to make comparison. By solving the Christoffel wave equation, the average sound velocity could be obtained from the angular average of the sound velocities calculated for each propagation direction, and consequently, the Thermo_pw package[31] allows the determination of the Debye temperature using the exact formula of v_D[16]. The obtained values of the average Debye sound velocity v_D are around 3.352 km/s for SrCuP and 2.597 m/s for SrCuSb compound, respectively. The Debye temperature is 361.5 K for SrCuP and 259 K for SrCuSb, respectively, which are in good agreement with the data obtained from Eq. (6).

The variation of Debye temperature θ_D as a function of pressure could be predicted using the following expression[17]:

$$\theta_D = \theta_{D_0}\left(\rho/\rho_0\right)^{\gamma} \tag{7}$$

where θ_{D0} is the Debye temperature obtained at ambient conditions, θ_D is the Debye temperature, γ is the Grüneisen parameter, ρ is the gravimetric density and ρ_0 is the gravimetric density obtained at ambient conditions. The Grüneisen parameter γ is an important thermodynamic quantity[47], which could be predicted using Vashchenko-Zubarev's formula, which is expressed as follows[48]:

$$\gamma_{V-Z} = \left(\frac{1}{2}B\prime + \frac{2}{9}\left(\frac{p}{\mathrm{B}}\right) - \frac{5}{6}\right) \Big/ \left(1 - \frac{4p}{3\mathrm{B}}\right) \tag{8}$$

where B and B' are the bulk modulus and its pressure derivative.

The variation of the Debye temperature θ_D as a function of pressure for both SrCuP and SrCuSb compounds is summarized in Table 5 and are shown in Fig. 5. The Debye temperature θ_D of both SrCuP and SrCuSb compounds increases gradually with increasing pressure. Similar qualitative behavior of θ_D versus pressure has been reported for both calcium oxide (CaO) compound[17] and MgCa intermetallic compound[45]. The best fit of our data on the Debye temperature θ_D (expressed in K) versus pressure p (expressed in GPa) are given by the following expressions: $\theta_D = 364.3 + 7.82p—0.15p^2$ for SrCuP and $\theta_D = 261.9 + 7.52p—0.2p^2$ for SrCuSb, respectively.

Furthermore, we evaluated the acoustic behavior of both SrCuP and SrCuSb materials by computing the acoustic impedance Z, which may be calculated by the following formula: $Z = (\rho G)^{1/2}$[49], where G is the shear modulus and ρ is the gravimetric density, respectively. The acoustic impedance Z of both SrCuP and SrCuSb

Parameter	v_l (km/s)	v_t (km/s)	v_m (km/s)	θ_D (K)	Z (Rayl)
SrCuP	5.123	3.051	3.377	364.2	14.61×10^6
SrCuSb	3.987 4.090[11]	2.369 2.472[11]	2.624 2.733[11]	261.8 272.5[11]	13.45×10^6

Table 4. Acoustic wave speeds, Debye temperature θ_D , and acoustic impedance Z for SrCuP and SrCuSb.

SrCuP	**p (GPa)**	**0**	**1.15**	**2.59**	**3.91**	**5.36**	**6.30**
	θ_D (K)	**364.3**	**373.1**	**383.5**	**392.6**	**402.0**	**407.8**
SrCuSb	p (GPa)	0	0.68	1.66	2.56	3.54	4.17
	θ_D (K)	261.8	266.9	273.8	279.8	286	289.8

Table 5. Debye temperature θ_D versus pressure p for SrCuP and SrCuSb compounds.

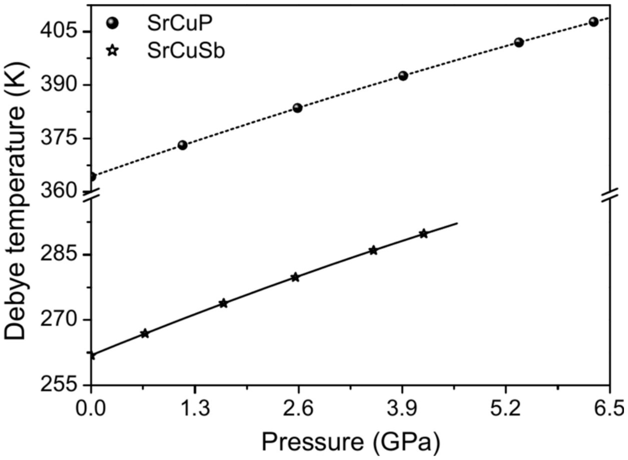

Fig. 5. Pressure dependence of Debye temperature for SrCuP and SrCuSb compounds in the BeZrSi type-structure.

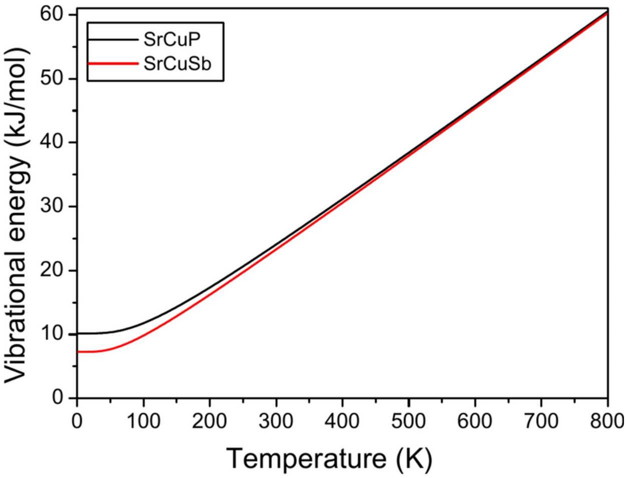

Fig. 6. Vibrational energy of phonons versus temperature for SrCuP and SrCuSb materials.

materials has been estimated at around 14.61×10^6 Rayl and 13.45×10^6 Rayl, respectively. They are slightly lower than the values 19.24×10^6 Rayl and 17.88×10^6 Rayl of Ti_2GaB and Zr_2GaB material, respectively[49].

Other thermodynamic properties

The temperature plays an influential role in determining the physical properties of materials[16]. The thermodynamic properties of both SrCuP and SrCuSb materials are theoretically predicted using the quasi-harmonic approximation. The detailed formulas used in the calculations of the thermodynamic properties of crystals are in the reference[50]. We report in Fig. 6 the vibrational energy of phonons as a function of temperature for both SrCuP and SrCuSb materials. The vibrational energy of phonons at room temperature (0 K) is about 25 kJ.mol^{-1} (10 kJ.mol^{-1}) for SrCuP and 22.5 kJ.mol^{-1} (6 kJ.mol^{-1}) for SrCuSb. A flat region is observed at low temperatures and an almost linear increase at high temperatures. This behavior predicted by our calculations is in agreement with a theoretical calculation for $LiMAl_2$ (M = Rh, Pd, Ir and Pt) materials[16], as well as for the tetragonal absorbent material Cu_2ZnSnS_4 (CZTS) in Kesterite phase[50], and for double quaternary perovskites

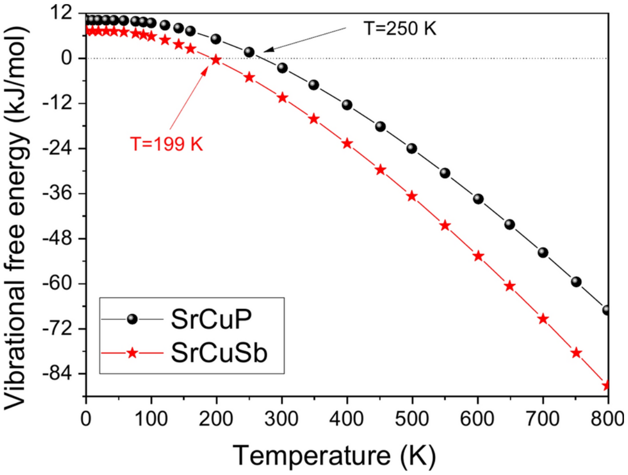

Fig. 7. The vibrational free energy versus temperature for SrCuP and SrCuSb materials.

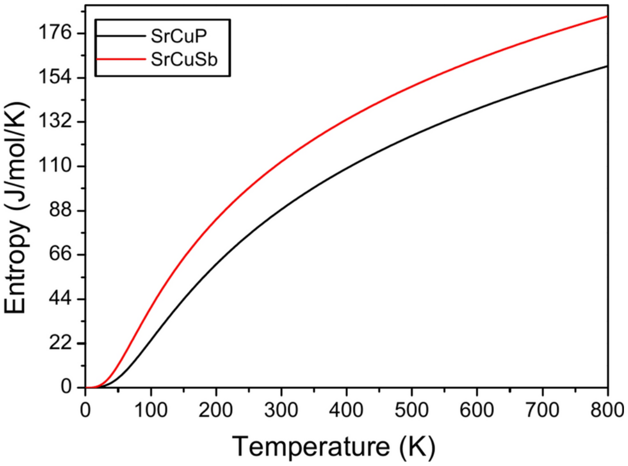

Fig. 8. Entropy versus temperature for SrCuP and SrCuSb compounds in the BeZrSi structure-type.

Ba_2NaHaO_6 (Ha = Cl, Br, I)[51]. At ambient temperature, the vibration energy of phonons has been found 24.14 kJ/mol and 23.37 kJ/mol for SrCuP and SrCuSb, respectively. The vibration free energy comes from a few low external modes, where their frequencies depend on the geometry and the adsorbed mass. At low frequencies, the energy curve is smooth because of the constant bond length. The vibrational free energy for both SrCuP and SrCuSb materials is illustrated in Fig. 7. At ambient temperature, the vibrational free energy is -2.58 kJ/mol for SrCuP and -10.49 kJ/mol for SrCuSb. There is a phase transition at 199 K and 250 K for SrCuSb and SrCuP respectively. We note that beyond these two temperatures, the two compounds are thermodynamically stable. This stability is more pronounced in SrCuSb. The free energy of vibration is positive when the chemicals are diatomic or larger.

The effect temperature on vibrational entropy S and the constant volume heat capacity C_V, with temperature ranging from 0 to 800 K for SrCuP and SrCuSb materials are shown in Figs. 8 and 9. As the temperature increases, both the entropy S and the heat capacity C_V increase as well. At low temperatures, one can observe that S increases quickly with rising the temperature.

At ambient temperature the entropy *S* is 88.81 $J.mol^{-1}.K^{-1}$ for SrCuP 112.54 $J.mol^{-1}.K^{-1}$ for SrCuSb; while the heat capacity at constant volume C_V is 69.83 $J.mol^{-1}.K^{-1}$ for SrCuP and 72.27 $J.mol^{-1}.K^{-1}$ for SrCuSb. The heat capacity for both SrCuP and SrCuSb materials increase rapidly under the lower temperature values from 0 to 200 K, above 200 K a slow increase in heat capacity can be seen, and the constant volume heat capacity approaches to the Dulong-Petit limit 75 $J.mol^{-1}.K^{-1}$, indicating that at high temperature all phonon modes are excited by the thermal energy[52–54]. The increase in temperature slightly affects the lattice parameters and fault structure[55]. Similar qualitative behavior has been reported for C_V versus temperature for heusler Mn_2NiGe ternary compound[10], for $LiMAl_2$ (M = Rh, Pd, Ir and Pt) materials[16], for tetragonal Cu_2ZnSnS_4 (CZTS) material in Kesterite phase[50], for scandium mono-phosphide (ScP) semiconductor[53], for cubic ZnS-type structure boron antimonide (BSb) compound[54], for cubic MgCu intermetallic compound[56], for cubic AuX_2 (X = Al, Ga, In) intermetallic compounds[57] and for cubic copper iodide (CuI) binary compound[58].

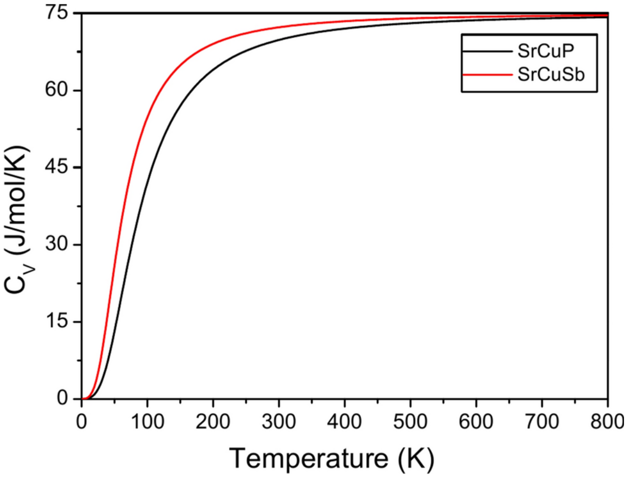

Fig. 9. Temperature dependence of the constant heat capacity for SrCuX (X = P, Sb) compounds.

Conclusion

In conclusion, an *ab-initio* projected augmented wave pseudopotentials method, based on the DFT has been employed to investigate the structural properties of both SrCuP and SrCuSb materials. Our findings on the lattice constants of our materials of interest are in agreement with the experimental data of the literature. We also report the calculation of the elastic constants and the thermodynamic properties for the first time to our knowledge in the case of both SrCuP and SrCuSb compounds. The calculated values of the Young modulus *E* for the aggregate materials are around 109.25 GPa for SrCuP compound and 78.22 GPa for SrCuSb, respectively. For our materials of interest, our calculated data on the thermodynamic properties show that all these quantities change monotonically with increasing temperature from 0 to 800 K. The Debye temperatures calculated based on elastic constants of SrCuP and SrCuSb compounds are 364.2 K and 261.8 K, respectively, and SrCuP exhibits higher stiffness (Young modulus) and better thermal conductivity for the higher Debye temperature. A critical aspect of this work was the dynamical stability check, which confirmed that both SrCuP and SrCuSb maintain stability under varying conditions, making them viable candidates for practical applications. The results presented here form a robust theoretical foundation for further experimental studies and optimization of SrCuX (X = P, Sb) materials for advanced thermoelectric devices.

Data Availability Statement

Data Availability Statement: Data underlying the results presented in this paper are not publicly available at this time but may be obtained from the author (fatmimessaoud@yahoo.fr) upon reasonable request.

Received: 22 November 2024; Accepted: 28 January 2025

References

1. Barreteau, C., Crivello, J.-C., Joubert, J.-M. & Alleno, E. Looking for new thermoelectric materials among TMX intermetallics using high-throughput calculations. *Comput. Mater. Sci.* **156**, 96–103 (2019).
2. Acharya, N., Fatima, B., Chouhan, S. S. & Sanyal, S. P. First principles study on structural, electronic, elastic and thermal properties of equiatomic MTi (M = Fe Co, Ni). *Chem. Mater. Res.* **3**(8), 22–30 (2013).
3. Mewis, A. ABX compounds with the structure Ni_2In: Preparation and crystal structure of CaCuP(As), SrCuP(As), SrAgP(As), and EuCuAs. *Z. fürNaturforsch. B* **33**, 983–986 (1978).
4. Eisenmann, B., Cordier, G. & Schäfer, H. CaCuSb(Bi) and SrCuSb(Bi) - ternary phases in the Filled NiAs-(Ni_2In)-structure. *Z. fürNaturforsch. B* **29**, 457–459 (1974).
5. Moll, A. et al. SrCuP and SrCuSb Zintl phases as potential thermoelectric materials. *J. Alloys Compd.* **942**, 169123 (2023).
6. Quinn, R. J. & Bos, J.-W.G. Recent progress in phosphide materials for thermoelectric conversion. *J. Mater. Chem. A* **11**, 8453–8469 (2023).
7. Jain, A. et al. Commentary: the Materials Project: a materials genome approach to accelerating materials innovation. *Apl Mater.* **1**, 011002 (2013).
8. R. J. Quinn, and J-W. G. Bos, Advances in half-Heusler alloys for thermoelectric power generation, *Mater. Adv.* 2 (2021) 6246–6266.
9. Zheng, S. et al. Planar Zintl-phase high-temperature thermoelectric materials XCuSb (X = Ca, Sr, Ba) with low lattice thermal conductivity. *J. Adv. Ceram.* **11**, 1604–1612 (2022).
10. Masrour, R. et al. Study of structural, elastic, thermal, electronic and magnetic properties of heusler Mn_2NiGe: An Ab initio calculations and Monte Carlo simulations. *Mater. Today Commun.* **26**, 101772 (2021).
11. Rima, A. N., Rahman, M. A., Ferdous, R., Nobin, M. N. M. & Rahman, M. F. DFT simulation to study the physical properties of ternary intermetallic materials ACuSb (A= Ca, Sr, Ba) for solar cell and TBC materials. *Comput. Condensed Matter.* **39**, e00900 (2024).
12. Benamrani, A., Rekab-Djabri, H., Bouarissa, N. & Daoud, S. Pressure-induced effects on the mechanical and thermophysical properties of $LiAl_2X$ (X = Rh, Pd, Ir and Pt) ternary intermetallic compounds. *Bull. Mater. Sci.* **47**, 52 (2024).

13. Qin, H., Luan, X., Feng, C., Yang, D. & Zhang, G. Mechanical, thermodynamic and electronic properties of wurtzite and zinc-blende GaN crystals. *Materials* **10**, 1419 (2017).
14. Mallah, A., Debbichi, M., Dhaou, M. H. & Bellakhdhar, B. Structural, mechanical, electronic, optical, and thermodynamic properties of new oxychalcogenide $A_2O_2B_2Se_3$ (A = Sr, Ba; B = Bi, Sb) compounds: A first-principles study. *Crystals* **13**, 122 (2023).
15. Ahmed, T. et al. Physical properties of rare earth perovskites CeMO3 (M= Co, Cu) in the context of density functional theory. *Mater. Today Commun.* **29**, 102973 (2021).
16. Benamrani, A., Daoud, S. & Bouarissa, N. First-principles study of structural, elastic and thermodynamic properties of $LiAl_2X$ (X= Rh, Pd, Ir, and Pt) intermetallic compounds. *Eur. Phys. J. B* **95**, 106 (2022).
17. Bioud, N. & Benchiheub, N. Pressure effect on some physical properties of calcium oxide material. *Chem. Phys. Impact* **7**, 100342 (2023).
18. Mahammed, M. A. & Mohammed, H. B. Variation of bulk modulus, its first pressure derivative, and thermal expansion coefficient with applied high hydrostatic pressure. *Adv Condensed Matter. Phys.* **2023**, 9518475 (2023).
19. Zeier, W. G. et al. Thinking like a chemist: intuition in thermoelectric materials. *Angew. Chem. Int. Ed.* **55**, 6826–6841 (2016).
20. Tambunan, O. T. et al. Thermoelectric properties of polycrystalline tetragonal SrCu2O2. *J. Ceramic Process. Res.* **12**(6), 673–676 (2011).
21. Raïâ, M. Y. et al. Thermodynamic, electronic, magnetic, thermoelectric, and optical properties of full Heuslers compounds Co_2TiAl(Ga, In): A First principles study. *Appl. Phys. A* **129**, 493 (2023).
22. Raïâ, M. Y. et al. Half-metalicity, mechanical, optical, thermodynamic, and thermoelectric properties of full Heusler alloys Co_2TiZ (Z = Si; Ge; Sn). *Opt. Quant. Electron.* **55**(6), 512 (2023).
23. Azouaoui, A. et al. First-principle investigation of LiSrX (X=P and As) half-Heusler semiconductor compounds, *Indian. J. Phys.* **97**, 1727–1737 (2023).
24. Raïâ, M. Y. et al. Stability, magnetic, electronic, elastic, thermodynamic, optical, and thermoelectric properties of Co_2TiSn, Co_2ZrSn and Co_2HfSn Heusler alloys from calculations using generalized gradient approximation techniques. *J. Mater. Sci: Mater. Electron.* **33**, 20229–20256 (2022).
25. Raïâ, M. Y. et al. Structural stability, electronic, magnetic, elastic, thermal, thermoelectric and optical properties of $L2_1$ and XA phases of Ti_2FeGe Heusler compound: GGA and GGA + U methods. *Nano. Micro. Thermo. Eng.* **27**(1), 1–24 (2023).
26. Raïâ, M. Y. et al. Effect of $L2_1$ and XA ordering on structural, martensitic, electronic, magnetic, elastic, thermal and thermoelectric properties of Co_2FeGe Heusler alloys. *Sol. Stat. Commun.* **355**(45), 114932 (2022).
27. Raïâ, M. Y. et al. Structural, electronic, magnetic, elastic, thermoelectric, and thermal properties of Co2FeGa1−xSix heusler alloys: First-principles calculations. *J. Supercond. Nov. Magn.* **36**, 349–365 (2023).
28. Elkoua, I. A. & Masrour, R. Structural, thermodynamics, optical, electronic, magnetic and thermoelectric properties of Heusler Ni_2MnGa: An ab initio calculation. *Opt. Quant. Electron.* **54**, 667 (2022).
29. Giannozzi, P. et al. QUANTUM ESPRESSO: A modular and open-source software project for quantum simulations of materials. *J. Phy. Condens. Matter* **21**, 395502 (2009).
30. Giannozzi, P. et al. Advanced capabilities for materials modelling with QUANTUM ESPRESSO. *J. Phys. Condens. Matter* **29**, 465901 (2017).
31. Corso, A. D. Elastic constants of beryllium: A first-principles investigation. *J. Phy. Condens. Matter* **28**, 075401 (2016).
32. Hamann, D. R. Optimized norm-conserving Vanderbilt pseudopotentials. *Phys. Rev. B* **88**, 085117 (2013).
33. Perdew, J. P., Burke, K. & Ernzerhof, M. Generalized gradient approximation made simple. *Phys. Rev. Lett.* **77**, 3865 (1996).
34. Monkhorst, H. J. & Pack, J. D. Special points for Brillouin-zone integrations. *Phys. Rev. B* **13**, 5188 (1976).
35. Broyden, C. G. The Convergence of a class of double-rank minimization algorithms 1. *General considerations. J. Inst. Math. Appl.* **6**, 222–231 (1970).
36. Fletcher, R. A new approach to variable metric algorithms. *Comput. J.* **13**, 317–322 (1970).
37. Goldfarb, D. A family of variable-metric methods derived by variational means. *Math. Comput.* **24**, 23–26 (1970).
38. Shanno, D. F. Conditioning of quasi-Newton methods for function minimization. *Math. Comput.* **24**, 647–656 (1970).
39. Shanno, D. F. An example of numerical nonconvergence of a variable-metric method. *J. Optimiz. Theor Appl.* **46**, 87–94 (1985).
40. Ghebouli, M. A., Ghebouli, B., Chihi, T. & Fatmi, M. Study of structural, elastic, electronic, dynamical and optical properties of beryllium selenide (BeSe) semiconductor in zinc blend and NiAs phases. *Physica B: Condensed Matter.* **610**, 412858 (2021).
41. Krache, L. et al. Phase stability, electronic, and optical properties in *Pcca*, *R3c*, and *Pm-3m* phases of $BiGaO_3$ perovskite. *Phys. Status Solidi B* **259**(10), 2200042 (2022).
42. Adachi, S. *Properties of Group-IV, III-V and II-VI Semiconductors* (John Wiley & Sons, 2005).
43. Amari, S., Rekab-Djabri, H. & Daoud, S. Mechanical, thermal, electronic, and magnetic properties of Ca0.75Er0.25S alloy from a DFT approach: A promising material for spintronic applications. *Mater. Today Commun.* **33**, 104237 (2022).
44. Amari, S. & Daoud, S. Structural phase transition, elastic constants and thermodynamic properties of TmAs: An ab-initio study. *Comput. Condens. Matter* **33**, e00764 (2022).
45. Daoud, S., Bouarissa, N., Benmakhlouf, A. & Allaoui, O. High-pressure effect on elastic constants and their related properties of MgCa intermetallic compound. *Phys. Status Solidi B* **257**, 1900537 (2020).
46. Rekab-Djabri, H. et al. Ground state parameters, electronic properties and elastic constants of $CaMg_3$: DFT study. *J. Magnes. Alloy.* **8**, 1166 (2020).
47. Amari, S., Daoud, S. & Rekab-Djabri, H. Structural, thermodynamic and magneto-electronic properties of Cd0.75Cr0.25Se and Zn0.75Cr0.25S: An ab-initio study. *Acta Phys. Pol. A* **143**(1), 36–46 (2023).
48. Okba, F. & Mezouar, R. Some physical parameters of calcium chalcogenides at high pressures: Semi-empirical approach. *J. Nano-Electron. Phys.* **14**(4), 04004 (2022).
49. Islam, S. et al. A comprehensive exploration of the physical properties of M_2GaB (M = Ti, Zr, Mo, Hf) through DFT method. *Results Mater.* **19**, 100438 (2023).
50. Boutahar, L., Benamrani, A., Rouabah, Z. & Daoud, S. Structural and thermodynamic properties of Cu_2ZnSnS_4material: Theoretical prediction. *Ann. West Univ. Timisoara Phys.* **65**, 160–170 (2023).
51. Rehman, Z. U. & Lin, Z. First-principles investigation of the structural stability, electronic, and thermodynamic properties of Ba2NaHaO6 (Ha = Cl, Br, I) periodate double perovskites. *J. Mater. Chem A* **12**, 8846–8861 (2024).
52. Bioud, N., Kassali, K. & Bouarissa, N. Thermodynamic properties of compressed CuX (X = Cl, Br) compounds: Ab initio study. *J. Electron Mater.* **46**, 2521–2528 (2017).
53. Benamrani, A., Daoud, S. & Saini, P. K. Structural, elastic and thermodynamic properties of ScP compound: DFT study. *J. Nano-Electron. Phys.* **13**(1), 01008 (2021).
54. Bioud, N., Sun, X. W., Daoud, S., Song, T. & Liu, Z. J. Structural stability and thermodynamic properties of BSb under high pressure and temperature. *Mater. Res. Express* **5**, 085904 (2018).
55. Böer, K. W. & Pohl, U. W. *Semiconductor Physics* (Springer International Publishing AG, 2018).
56. Daoud, S., Bioud, N. & Saini, P. K. Finite temperature thermophysical properties of MgCu intermetallic compound from quasi-harmonic Debye model. *J. Magn. Alloys* **7**, 335 (2019).
57. Dar, S. A., Srivastava, V., Tripathi, S. N. & Sakalle, U. K. A complete DFT description on structural, electronic, elastic, mechanical and thermodynamic properties of some intermetallic AuX2 (X = Al, Ga, In) compounds. *Eur. Phys. J. Plus* **133**, 541 (2018).
58. Bioud, N. et al. High-pressure phase transition and thermodynamic properties from first-principles calculations: Application to cubic copper iodide. *Mater. Chem. Phys.* **203**, 362 (2018).

Acknowledgements

The authors extend their appreciation to the Deanship of Scientific Research at Northern Border University, Arar, KSA for funding this research work through the project number NBU-FFR-2025-310-06.

Author contributions

Conceptualization: N. Bioud Data curation: N. Benchiheub Formal analysis: A. Benamrani Methodology: M.A. Ghebouli, R. Yekhlef Validation: M. Fatmi, Faisal Katib Alanazi.

Declarations

Competing interests

The authors declare no competing interests.

Additional information

Correspondence and requests for materials should be addressed to N.B., M.F. or F.K.A.

Reprints and permissions information is available at www.nature.com/reprints.

Publisher's note Springer Nature remains neutral with regard to jurisdictional claims in published maps and institutional affiliations.

Open Access This article is licensed under a Creative Commons Attribution-NonCommercial-NoDerivatives 4.0 International License, which permits any non-commercial use, sharing, distribution and reproduction in any medium or format, as long as you give appropriate credit to the original author(s) and the source, provide a link to the Creative Commons licence, and indicate if you modified the licensed material. You do not have permission under this licence to share adapted material derived from this article or parts of it. The images or other third party material in this article are included in the article's Creative Commons licence, unless indicated otherwise in a credit line to the material. If material is not included in the article's Creative Commons licence and your intended use is not permitted by statutory regulation or exceeds the permitted use, you will need to obtain permission directly from the copyright holder. To view a copy of this licence, visit http://creativecommons.org/licenses/by-nc-nd/4.0/.

© The Author(s) 2025